FACTA UNIVERSITATIS
Series: **Mechanics, Automatic Control and Robotics** Vol.4, N° 16, 2004, pp. 141 - 156

A NUMERICAL APPROACH TO ANALYSIS OF AXISYMMETRIC RINGS

UDC 537.226.96.(045)

Dragan Mančić, Milan Radmanović

Faculty of Electronic Engineering, University of Niš, A. Medvedeva 14, 18000 Niš, Serbia and Montenegro
E-mail: dmancic@elfak.ni.ac.yu, radmanovic@ni.ac.yu

Abstract. *In this paper, using the exact three-dimensional equations of linear elasticity, the axisymmetric vibrations of a finite solid circular ring of various hole and length have been studied. The real, imaginary and complex branches of the corresponding dispersion spectra, obtained by satisfying the stress-free boundary conditions exactly at the lateral surface of the ring have been superposed to satisfy, approximately, the stress-free boundary conditions at the flat surfaces of the ring. The process of superposition yields a transcendental equation, which gives the frequency-length curves for the ring. These curves have been given for rings with various materials and for different selected dimensions.*

Key words: *Frequency equation, Numerical method, Resonance frequency*

INTRODUCTION

The studies of vibrations in axisymmetric hollow cylinders of finite length (axisymmetric rings) are often related to practical problems. In general, we will have to solve the three-dimensional equations of the linear theory of elasticity when we want to study vibrations of elastic rings. The solution of the elastic equations has proved to be a challenging task that has produced the approaches that differ in the extent of the assumptions made and in the extent to which the solution is taken.

This paper, motivated by the use of metal and piezoceramic rings with ultrasonic sandwich transducers [1], presents a complete solution of the elastic equations for freely supported axisymmetric rings, according to theory of vibrations for finite isotropic elastic shells [2]. In this paper the exact differential equations are used, but the boundary conditions are satisfied approximately. The solution is obtained considering all roots of the frequency equation (real, imaginary and complex), when the boundary conditions are satisfied. The numerical results obtained allow prediction of the various modes of vibration possible for axisymmetric rings as a function of the ring dimensions. Additionally, numerical results are

Received July 30, 2003

extended to the case of piezoceramic rings, where a piezoceramic ring having such a large elastic anisotropy can be approximated by the theory for an isotropic rings, without consideration of the piezoelectric properties of rings.

2. FORMULATION OF THE PROBLEM

The Lame's partial differential equation for a homogenous, isotropic elastic material, written in terms of displacements and in vector notation, take the form [3]:

$$\rho\frac{\partial^2\mathbf{u}}{\partial t^2} = (\lambda_m + \mu)\,\mathrm{graddiv}\mathbf{u} + \mu\nabla^2\mathbf{u} \quad , \tag{1}$$

where λ_m, μ are the two Lame's constants characterizing the solid, t is the time, ρ is the material density, and $\boldsymbol{u}$ is the displacement vector associated with an elementary volume of the material. ∇ is defined by Eq. (2):

$$\nabla^2 = \left(\frac{\partial^2}{\partial r^2} + \frac{1}{r}\frac{\partial}{\partial r}\right), \tag{2}$$

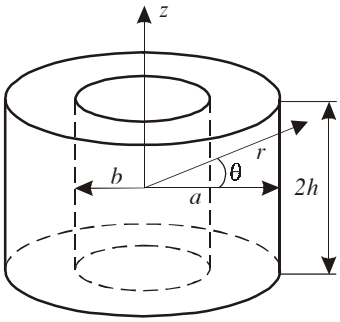

Fig. 1. Notation in cylindrical coordinates

where r is the radial distance from origin located at the ring center. This paper is concerned with circular rings and consequently cylindrical coordinates r, θ, z are chosen with the z direction coincident with the axis of the ring (Fig. 1). The central plane of the ring is assumed to be located at $z = 0$ so that the plane ends of the ring lie at $z = \pm h$.

The detailed notation for the geometrical and physical parameters of the ring follows. h, a and b denote the half-length, outer and inner radii of the ring, respectively. We denote υ as Poisson's ratio, E_Y as Young's modulus, $\lambda_m = (\upsilon E_Y)/((1+\upsilon)(1-2\upsilon))$ and $\mu = E_Y/2(1+\upsilon)$ as Lame's constants. $v_d = \sqrt{(\lambda_m + 2\mu)/\rho}$ and $v_s = \sqrt{\mu/\rho}$ are velocities of dilatational and shear waves, respectively, in infinite media [3].

The angular frequency ω is 2π times the frequency, $k = 2\pi/\lambda$ is the propagation constant or wavenumber and λ is the wavelength. The dimensionless quantities are introduced as follows: $\Omega = \omega a/v_s$ is the normalized frequency and $\xi = k\,a$ is the normalized propagation constant. u_r, u_θ, u_z denote the components of the displacement vector in the radial, tangential and axial directions, respectively. T_{rr}, T_{rz} and T_{zz} are the components of the stress tensor.

With the assumption that tangential displacements in the θ direction u_θ are zero (axisymmetric vibrations), the vector equation (1) expands to yield the two equations:

$$\rho\frac{\partial^2 u_r}{\partial t^2}=(\lambda_m+2\mu)\frac{\partial}{\partial r}\left(\frac{\partial u_r}{\partial r}+\frac{u_r}{r}\right)+(\lambda_m+\mu)\frac{\partial^2 u_z}{\partial r\partial z}+\mu\frac{\partial^2 u_r}{\partial z^2},$$
$$\rho\frac{\partial^2 u_z}{\partial t^2}=(\lambda_m+\mu)\frac{\partial}{\partial z}\left(\frac{\partial u_r}{\partial r}+\frac{u_r}{r}\right)+(\lambda_m+2\mu)\frac{\partial^2 u_z}{\partial z^2}+\mu\left(\frac{\partial^2 u_z}{\partial r^2}+\frac{1}{r}\frac{\partial u_z}{\partial r}\right), \tag{3}$$

where u_r and u_z are the radial and axial displacements, respectively.

For axially symmetric motion, the solutions of Eqs. (3) are given by the following [4]:

$$u_r=\left[-A\frac{\partial J_0(\alpha r)}{\partial r}-B\frac{\partial Y_0(\alpha r)}{\partial r}+Ck\frac{\partial J_0(\beta r)}{\partial r}+Dk\frac{\partial Y_0(\beta r)}{\partial r}\right]e^{j(\omega t-kz)},$$
$$u_z=j[AkJ_0(\alpha r)+BkY_0(\alpha r)+C\beta^2 J_0(\beta r)+D\beta^2 Y_0(\beta r)]\,e^{j(\omega t-kz)}, \tag{4}$$

where A, B, C and D are arbitrary constants, J_i and Y_i are the first and the second kind of Bessel's functions of the order i and

$$\alpha^2=(\omega^2/v_d^2)-k^2,\qquad \beta^2=(\omega^2/v_s^2)-k^2. \tag{5}$$

Eqs. (4) include two types of motions, one of which is symmetric about the central plane of the ring ("symmetric motion"), whereas the other is antisymmetric ("antisymmetric motion"). For symmetric motion the term e^{-jkz} with u_r and je^{-jkz} with u_z will be replaced by cos kz and sin kz respectively whereas for antisymmetric motion, u_r and u_z will have sin kz and cos kz, respectively.

The unknown coefficients A, B, C and D are determined by application of the boundary conditions that the ring lateral surfaces are stress-free. In other words, the ring under consideration is to be freely supported and consequently the normal stress in the radial direction (T_{rr}) and shear (tangential) stress (T_{rz}) at the lateral surfaces must vanish:

$$(T_{rr})_{r=a}=0,\ \text{for all } z \text{ and } t,$$
$$(T_{rz})_{r=a}=0,\ \text{for all } z \text{ and } t,$$
$$(T_{rr})_{r=b}=0,\ \text{for all } z \text{ and } t,$$
$$(T_{rz})_{r=b}=0,\ \text{for all } z \text{ and } t,$$

where the components of the stress tensor are [3]:

$$T_{rr}=\lambda_m\left(\frac{\partial u_r}{\partial r}+\frac{u_r}{r}+\frac{\partial u_z}{\partial z}\right)+2\mu\frac{\partial u_r}{\partial r},$$
$$T_{rz}=\mu\left(\frac{\partial u_r}{\partial z}+\frac{\partial u_z}{\partial r}\right), \tag{7}$$
$$T_{zz}=\lambda_m\left(\frac{\partial u_r}{\partial r}+\frac{u_r}{r}+\frac{\partial u_z}{\partial z}\right)+2\mu\frac{\partial u_z}{\partial z}.$$

Substitution of Eqs. (4) into Eqs. (6) leads to four homogenous equations in the terms of the unknown's coefficients A, B, C and D. The only nontrivial solutions for A, B, C and

D are those for which the determinant of the coefficients of A, B, C and D is equal to zero. This determinant is:

$$\begin{vmatrix} A_{11} & A_{12} & A_{13} & A_{14} \\ A_{21} & A_{22} & A_{23} & A_{24} \\ A_{31} & A_{32} & A_{33} & A_{34} \\ A_{41} & A_{42} & A_{43} & A_{44} \end{vmatrix} = 0 , \tag{8}$$

where:

$$A_{11} = (\xi^2 - \Omega^2/2)\ J_0(\alpha a) + (\alpha a) J_1(\alpha a),$$
$$A_{12} = (\xi^2 - \Omega^2/2)\ Y_0(\alpha a) + (\alpha a) Y_1(\alpha a),$$
$$A_{13} = \xi [(\beta a)\ J_0(\beta a) - J_1(\beta a)],$$
$$A_{14} = \xi [(\beta a)\ Y_0(\beta a) - Y_1(\beta a)],$$
$$A_{21} = -2\xi (\alpha a)\ J_1(\alpha a),$$
$$A_{22} = -2\xi (\alpha a)\ Y_1(\alpha a),$$
$$A_{23} = (2\xi^2 - \Omega^2)\ J_1(\beta a),$$
$$A_{24} = (2\xi^2 - \Omega^2)\ Y_1(\beta a),$$
$$A_{31} = (b/a)^2 (\xi^2 - \Omega^2/2)\ J_0(\alpha b) + (\alpha b) J_1(\alpha b),$$
$$A_{32} = (b/a)^2 (\xi^2 - \Omega^2/2)\ Y_0(\alpha b) + (\alpha b) Y_1(\alpha b),$$
$$A_{33} = \xi (b/a) [(\beta b)\ J_0(\beta b) - J_1(\beta b)],$$
$$A_{34} = \xi (b/a) [(\beta b)\ Y_0(\beta b) - Y_1(\beta b)],$$
$$A_{41} = -2\xi (b/a)(\alpha b)\ J_1(\alpha b),$$
$$A_{42} = -2\xi (b/a)(\alpha b)\ Y_1(\alpha b),$$
$$A_{43} = (b/a)^2 (2\xi^2 - \Omega^2)\ J_1(\beta b),$$
$$A_{44} = (b/a)^2 (2\xi^2 - \Omega^2)\ Y_1(\beta b).$$

The equation formed by expanding Eq. (8) is the so-called frequency equation, which relates to the dimensionless variables Ω and ξ, with Young's modulus E_Y, Poisson's ratio υ and inner radius to outer radius ratio b/a as parameters. For a particular set of the physical parameters E_Y, υ and geometrical parameter b/a, the characteristic Eq. (8) involves only the frequency parameter Ω and the non-dimensional wavenumber ξ. From physical considerations, the frequency parameter Ω is real but the wavenumber ξ can be real, imaginary or complex. The $\Omega = f(\xi)$ curves for the real, imaginary and complex values of ξ will, hereinafter, be referred to as "real branch", "imaginary branch" and "complex branch" of the dispersion spectra, respectively. At a particular frequency, there are a finite number of real and imaginary branches and an infinite number of complex branches.

In this paper, we construct the real, imaginary and complex branches to various rings with materials and dimensions usually used in power ultrasonic sandwich transducers. The numerical evaluation of the roots of Eq. (8) is obtained using high-speed computer.

By numerical modeling of axisymmetric rings the program for computation of Eq. (8) was generated and can be seen in Appendix A. In this way, nine branches were computed for duralumin, steel and PZT8 rings. These various physical and geometrical parameters are chosen as follows (Table 1) [5], [6]:

Table 1. Characteristics of the used metal and piezoceramic rings

	duralumin	steel	PZT8
a (mm)	20	20	19
b (mm)	4	4	7.5
υ	0.34	0.29	0.3
E_Y (Pa)	$0.74 \cdot 10^{11}$	$2.18 \cdot 10^{11}$	$0.74 \cdot 10^{11}$
ρ (kg/m^3)	2790	7850	7600
v_d (m/s)	6389	6033	3622
v_s(m/s)	3146	3281	1936

These branches are shown in Figs. 2, 3 and 4, respectively, as an extension of the numerical results presented for empty and fluid-filled cylindrical shells [2], [4]. The dispersion spectra are constructed for the following ranges of Ω, ξ and b/a: $0 \le \Omega \le 10$, $0 \le |\xi| \le 14$, $b/a = 0.2$ for metal duralumin and steel rings (Fig. 2 and 3) and $0 \le \Omega \le 30$, $0 \le |\xi| \le 15$, $b/a = 0.2$ for PZT8 piezoceramic ring (Fig. 4).

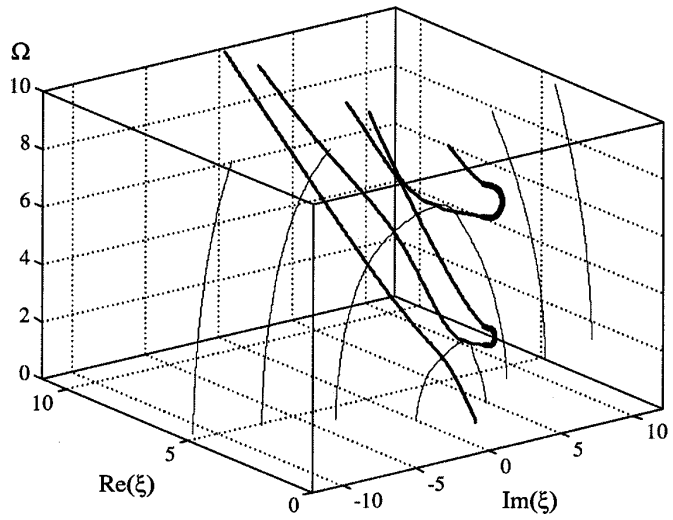

Fig. 2. Normalized resonant frequency Ω as a function of propagation constant ξ for duralumin ring using Eq. (8):
—— real branch, ▬▬ imaginary branch, —— complex branch

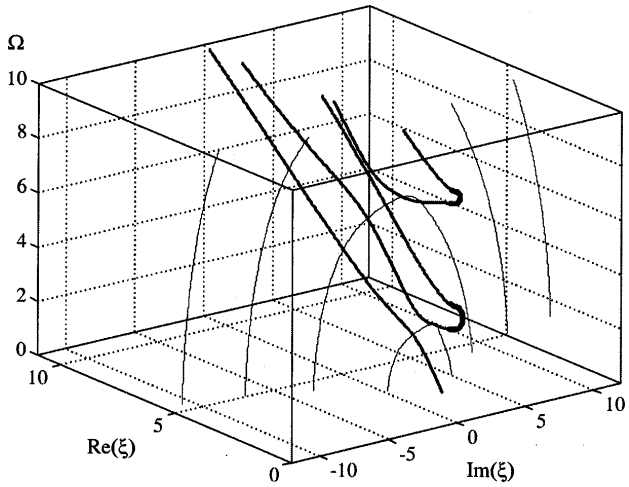

Fig. 3. Normalized resonant frequency Ω as a function of propagation constant ξ for steel ring using Eq. (8):
—— real branch, ▬▬ imaginary branch, —— complex branch

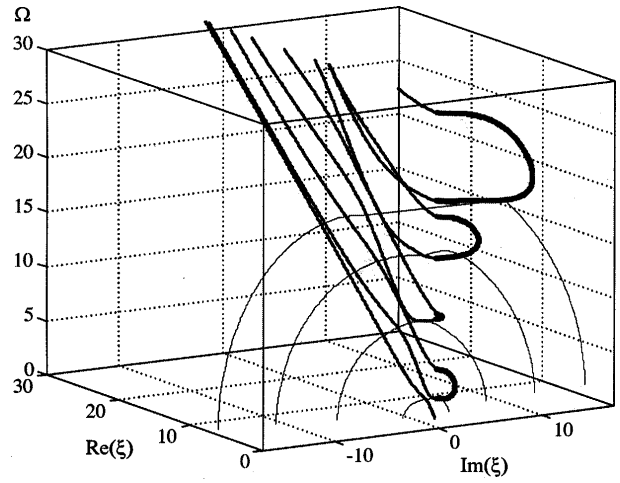

Fig. 4. Normalized resonant frequency Ω as a function of propagation constant ξ for PZT8 ceramic ring using Eq. (8):
—— real branch, ▬▬ imaginary branch, —— complex branch

3. BOUNDARY CONDITIONS AT THE FLAT ENDS OF THE RING

The existence of multiple values of ξ for the same frequency Ω requires the individual motions corresponding to different values of ξ should be combined to get the resultant motion. The amplitudes of these motions could be properly adjusted to satisfy the boundary condition at the flat surfaces, as much as possible. If we consider ring with free ends,

stresses on these free boundary surfaces must be equal to zero. However, it is evident from Eqs. (7) that T_{rr} and T_{rz} cannot be simultaneously made zero for all values of r (i.e. at all point of the flat surfaces of the ring) because it requires the simultaneous vanishing of cos kz and sin kz at the same points. In this paper we have solved the problem by a method in which the boundary conditions are satisfied with better uniformity.

For a particular b/a, suppose the characteristic equation, obtained on satisfying exact boundary conditions at the lateral surfaces of the ring, gives $2m$+1 values of the wavenumber ξ at a specified frequency Ω (in our case nine values). The motions corresponding to these $2m$+1 wavenumbers are linearly superposed by introducing $2m$+1 arbitrary constants A_i. We, now, satisfy $2m$+1 boundary conditions at the flat ends of the ring by requiring either normal (T_{rr}) or shear (T_{rz}) stresses to vanish at $2m$+1 pre-selected locations. These conditions will give $2m$+1 simultaneous algebraic equations with $2m$+1 constants A_i. Therefore boundary conditions can be written in the form:

$$T_{zz} = \sum_{i=1}^{2m+1} A_i T_{zz\, i,\, rm1} = 0, \quad z = \pm h, \tag{10}$$

where $r_{m1}=b + m_1 (a-b) / m$, $m_1=0,1,2, \ldots m$, and

$$T_{rz} = \sum_{i=1}^{2m+1} A_i T_{rz\, i,\, rm2} = 0, \quad z = \pm h, \tag{11}$$

where $r_{m2}=b + m_2 (a-b) / (m+1)$, $m_2=1,2, \ldots m$.

$T_{zz\, i,\, rm1}$ and $T_{rz\, i,\, rm2}$ are the axial and shear stresses corresponding to i-th branch of the dispersion spectra and calculated at $r = r_{m1}$ or $r = r_{m2}$. A_i is the amplitude constant corresponding to i-th branch. T_{zz} and T_{rz} are the resultant axial and shear stresses respectively. Eqs. (10) and (11) represents a set of $2m + 1$ independent homogeneous equations involving A_i as the $2m + 1$ unknowns. For a non-zero solution, these equations give the following determinantal equation:

$$\Delta = \begin{vmatrix} T_{zz\,1,\,r_0} & T_{zz\,2,\,r_0} & \cdots & \cdots & T_{zz\,2m+1,\,r_0} \\ T_{zz\,1,\,r_1} & T_{zz\,2,\,r_1} & \cdots & \cdots & T_{zz\,2m+1,\,r_1} \\ \cdots & \cdots & \cdots & \cdots & \cdots \\ \cdots & \cdots & \cdots & \cdots & \cdots \\ T_{zz\,1,\,r_m} & T_{zz\,2,\,r_m} & \cdots & \cdots & T_{zz\,2m+1,\,r_m} \\ T_{rz\,1,\,r_1} & T_{rz\,2,\,r_1} & \cdots & \cdots & T_{rz\,2m+1,\,r_1} \\ T_{rz\,1,\,r_2} & T_{rz\,2,\,r_2} & \cdots & \cdots & T_{rz\,2m+1,\,r_2} \\ \cdots & \cdots & \cdots & \cdots & \cdots \\ \cdots & \cdots & \cdots & \cdots & \cdots \\ T_{rz\,1,\,r_m} & T_{rz\,2,\,r_m} & \cdots & \cdots & T_{rz\,2m+1,\,r_m} \end{vmatrix} = 0 . \tag{12}$$

For any particular resonant frequency $f = \omega/(2\pi)$ and particular ratio b/a, this determinantal equation becomes a transcendental equation in length l, as the only unknown pa-

rameter and gives an infinite set of values for the same. Transcendental equation is different for the symmetric and antisymmetric motions, and this paper is devoted to the discussion of both motions. In this paper, we have calculated the values of l for the symmetric and antisymmetric motions, falling in the range $0 < l < 120$mm, for the rings with parameters given in Table 1. The first three symmetric and antisymmetric f versus l curves for metal duralumin and steel rings have been obtained for roots of Eq. (12) within the range $0 \le f \le 180$kHz, for $b = 8$mm and $a = 40$mm. The first eight symmetric and the first antisymmetric f versus l curves for PZT8 ceramic ring have been plotted for roots of Eq. (12) within the range $0 \le f \le 300$kHz, for $b = 15$mm and $a = 38$mm. The variations of the frequency f with the length l for duralumin, steel and PZT8 rings have been plotted in Figs. 5, 6 and 7, respectively.

The numerical work was done on a computer using Mathematica programming language. The main program that makes use of formed algorithm is shown in Appendix B.

4. CONCLUSION

Presented figures show spectra complexity for small ring's thickness. Resonant frequency dependences versus duralumin and steel ring thickness (length), given at Figs. 5 and 6, show that rings with the same dimensions made of particular metals, have very similar resonant frequency spectra, as also given at Figs. 2 and 3. It is obvious that frequency of these modes don't decrease uniformly with thickness in the analyzed range of f and l, because in some areas appear terrace-type spectra due to modes coupling, where small changes of thickness cause a large frequency variation and vice versa. It is obvious at frequency region around 75kHz on Figs. 5 and 6, for the booth metal rings, where all branches have step-like structures. Also, it is frequency region where the first complex branch of dispersion spectra appears (Figs. 2 and 3). Moreover, near $f = 90$kHz the third mode have step-like structure, like higher modes which are not presented.

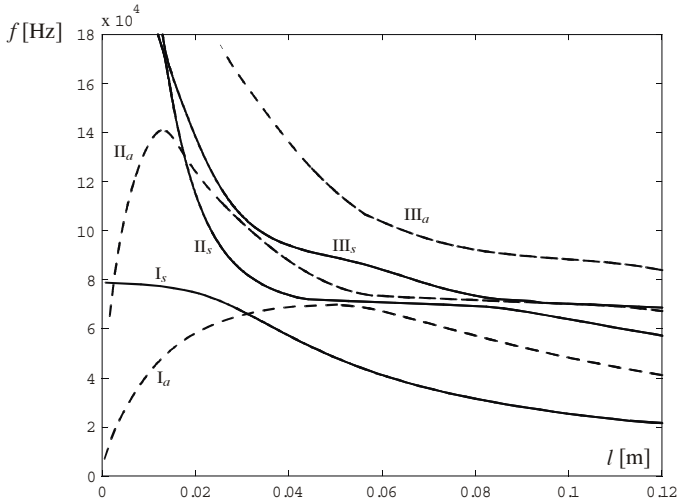

Fig. 5. Resonant frequency f as a function of length l for duralumin ring ($b/a = 0.2$): s – symmetric modes, a – antisymmetric modes

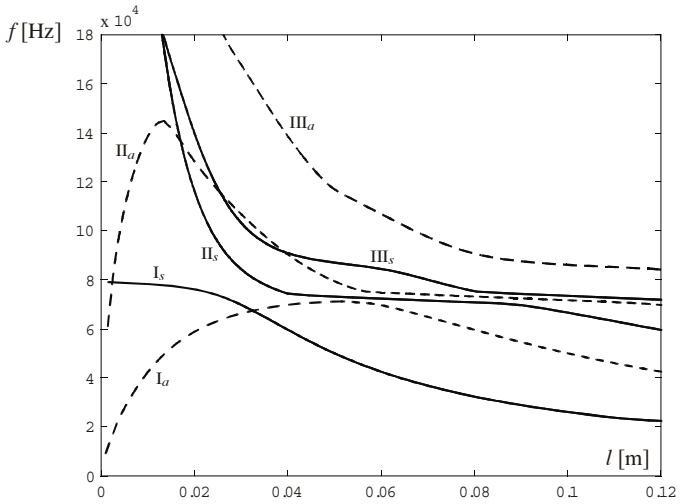

Fig. 6. Resonant frequency f as a function of length l for steel ring (b/a = 0.2): s – symmetric modes, a – antisymmetric modes

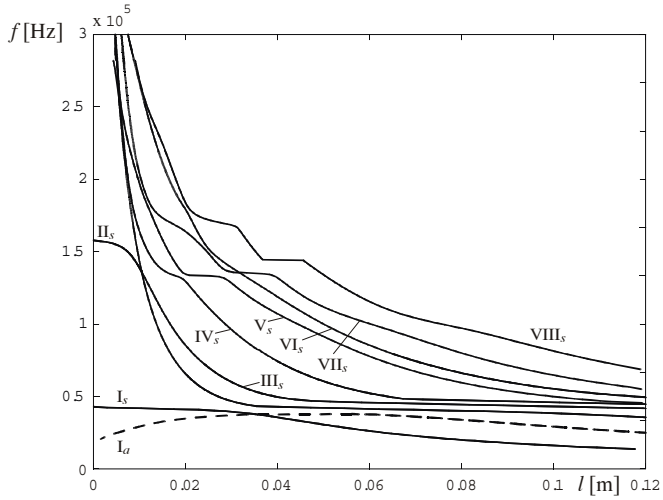

Fig. 7. Resonant frequency f as a function of length l for PZT8 ceramic ring (b/a = 0.4): s – symmetric modes, a – antisymmetric mode

The terrace-type parts of spectra are located at different frequency regions for PZT8 piezoceramic ring, i.e. near 45kHz, 140kHz and 170kHz, as a result of completely different dimensions and characteristics. It is very interesting to notice that frequency spectra of a ceramic ring having such a large elastic anisotropy can be approximated by the theory for an isotropic ring.

The method developed in this paper produces yielding results with a remarkably small amount of computational effort. This method is very useful to assist the designer to achieve a desired frequency characteristic. The proposed method is general, because for inner radius $b = 0$, previous numerical procedure gives solutions for full cylinder (or disc) vibrations [7].

APPENDIX A

The Mathematica code to determine the normalized frequency (Ω) versus the normalized propagation constant (ξ), for duralumin with radius ratio $b/a = 0.2$ (Fig. 2), is shown below:

```
CLEARALL[];

(*DURALUMIN D5*)
V=0.34;
EE=0.74*10^11;
RO=2790;

MI=EE/(2*(1+V));
LAM=(V*EE)/((1+V)*(1-2*V));

CS=SQRT[MI/RO];
CD=SQRT[(LAM+2*MI)/RO];
K1=CS/CD;
K2=0.2;
R=K2;

ALFAA[Q_,S_]=SQRT[Q^2*K1^2-S^2];
ALFAB[Q_,S_]=K2*ALFAA[Q,S];
BETAA[Q_,S_]=SQRT[Q^2-S^2];
BETAB[Q_,S_]=K2*BETAA[Q,S];

J0ALFAA[Q_,S_]=BESSELJ[0,ALFAA[Q,S]];
J1ALFAA[Q_,S_]=BESSELJ[1,ALFAA[Q,S]];
J0ALFAB[Q_,S_]=BESSELJ[0,ALFAB[Q,S]];
J1ALFAB[Q_,S_]=BESSELJ[1,ALFAB[Q,S]];
J0BETAA[Q_,S_]=BESSELJ[0,BETAA[Q,S]];
J1BETAA[Q_,S_]=BESSELJ[1,BETAA[Q,S]];
J0BETAB[Q_,S_]=BESSELJ[0,BETAB[Q,S]];
J1BETAB[Q_,S_]=BESSELJ[1,BETAB[Q,S]];

Y0ALFAA[Q_,S_]=BESSELY[0,ALFAA[Q,S]];
Y1ALFAA[Q_,S_]=BESSELY[1,ALFAA[Q,S]];
Y0ALFAB[Q_,S_]=BESSELY[0,ALFAB[Q,S]];
Y1ALFAB[Q_,S_]=BESSELY[1,ALFAB[Q,S]];
Y0BETAA[Q_,S_]=BESSELY[0,BETAA[Q,S]];
Y1BETAA[Q_,S_]=BESSELY[1,BETAA[Q,S]];
Y0BETAB[Q_,S_]=BESSELY[0,BETAB[Q,S]];
Y1BETAB[Q_,S_]=BESSELY[1,BETAB[Q,S]];

D11[Q_,S_]=(S^2-Q^2/2)*J0ALFAA[Q,S]+ALFAA[Q,S]*J1ALFAA[Q,S];
D12[Q_,S_]=(S^2-Q^2/2)*Y0ALFAA[Q,S]+ALFAA[Q,S]*Y1ALFAA[Q,S];
D13[Q_,S_]=S*(BETAA[Q,S]*J0BETAA[Q,S]-J1BETAA[Q,S]);
D14[Q_,S_]=S*(BETAA[Q,S]*Y0BETAA[Q,S]-Y1BETAA[Q,S]);
```

```
D21[Q_,S_]=-2*S*(ALFAA[Q,S]*J1ALFAA[Q,S]);
D22[Q_,S_]=-2*S*(ALFAA[Q,S]*Y1ALFAA[Q,S]);
D23[Q_,S_]=(2*S^2-Q^2)*J1BETAA[Q,S];
D24[Q_,S_]=(2*S^2-Q^2)*Y1BETAA[Q,S];

D31[Q_,S_]=R^2*(S^2-Q^2/2)*J0ALFAB[Q,S]+ALFAB[Q,S]*J1ALFAB[Q,S];
D32[Q_,S_]=R^2*(S^2-Q^2/2)*Y0ALFAB[Q,S]+ALFAB[Q,S]*Y1ALFAB[Q,S];
D33[Q_,S_]=(S*R)*(BETAB[Q,S]*J0BETAB[Q,S]-J1BETAB[Q,S]);
D34[Q_,S_]=(S*R)*(BETAB[Q,S]*Y0BETAB[Q,S]-Y1BETAB[Q,S]);

D41[Q_,S_]=-2*(S*R)*(ALFAB[Q,S]*J1ALFAB[Q,S]);
D42[Q_,S_]=-2*(S*R)*(ALFAB[Q,S]*Y1ALFAB[Q,S]);
D43[Q_,S_]=R^2*(2*S^2-Q^2)*J1BETAB[Q,S];
D44[Q_,S_]=R^2*(2*S^2-Q^2)*Y1BETAB[Q,S];

Y[Q_,S_]=
D11[Q,S]*D22[Q,S]*D33[Q,S]*D44[Q,S]-D11[Q,S]*D22[Q,S]*D34[Q,S]*D43[Q,S]-
D11[Q,S]*D32[Q,S]*D23[Q,S]*D44[Q,S]+D11[Q,S]*D32[Q,S]*D24[Q,S]*D43[Q,S]+
D11[Q,S]*D42[Q,S]*D23[Q,S]*D34[Q,S]-D11[Q,S]*D42[Q,S]*D24[Q,S]*D33[Q,S]-
D21[Q,S]*D12[Q,S]*D33[Q,S]*D44[Q,S]+D21[Q,S]*D12[Q,S]*D34[Q,S]*D43[Q,S]+
D21[Q,S]*D32[Q,S]*D13[Q,S]*D44[Q,S]-D21[Q,S]*D32[Q,S]*D14[Q,S]*D43[Q,S]-
D21[Q,S]*D42[Q,S]*D13[Q,S]*D34[Q,S]+D21[Q,S]*D42[Q,S]*D14[Q,S]*D33[Q,S]+
D31[Q,S]*D12[Q,S]*D23[Q,S]*D44[Q,S]-D31[Q,S]*D12[Q,S]*D24[Q,S]*D43[Q,S]-
D31[Q,S]*D22[Q,S]*D13[Q,S]*D44[Q,S]+D31[Q,S]*D22[Q,S]*D14[Q,S]*D43[Q,S]+
D31[Q,S]*D42[Q,S]*D13[Q,S]*D24[Q,S]-D31[Q,S]*D42[Q,S]*D14[Q,S]*D23[Q,S]-
D41[Q,S]*D12[Q,S]*D23[Q,S]*D34[Q,S]+D41[Q,S]*D12[Q,S]*D24[Q,S]*D33[Q,S]+
D41[Q,S]*D22[Q,S]*D13[Q,S]*D34[Q,S]-D41[Q,S]*D22[Q,S]*D14[Q,S]*D33[Q,S]-
D41[Q,S]*D32[Q,S]*D13[Q,S]*D24[Q,S]+D41[Q,S]*D32[Q,S]*D14[Q,S]*D23[Q,S];

N=307;
STEP=0.03;
S1=1.51+2.4*I;
Q=0.81;
FOR[I=1, I<=N, I++,
R=FINDROOT[Y[Q,S]==0,{S,S1}];
S1=S/.R;
S1>>>D:\RESULTS;
Q=Q+STEP;
PRINT[S1];
];
```

APPENDIX B

Below is the Mathematica program written to determine the first resonance frequency (f□) versus the length (l) of duralumin axisymmetric ring with b/a=0.2:

```
CLEARALL[];

(*DURALUMIN D5*)
V=0.34;
EE=0.74*10^11;
RO=2790;
MI=EE/(2*(1+V));
LAM=(V*EE)/((1+V)*(1-2*V));

CS=SQRT[MI/RO];
CD=SQRT[(LAM+2*MI)/RO];
K=(CD/CS)^2-2;
K1=CS/CD;
K2=0.2;
R=K2;
```

```
ALFAA[Q_,S_]=SQRT[Q^2*K1^2-S^2];
ALFAB[Q_,S_]=K2*ALFAA[Q,S];
BETAA[Q_,S_]=SQRT[Q^2-S^2];
BETAB[Q_,S_]=K2*BETAA[Q,S];

J0ALFAA[Q_,S_]=BESSELJ[0,ALFAA[Q,S]];
J1ALFAA[Q_,S_]=BESSELJ[1,ALFAA[Q,S]];
J0ALFAB[Q_,S_]=BESSELJ[0,ALFAB[Q,S]];
J1ALFAB[Q_,S_]=BESSELJ[1,ALFAB[Q,S]];
J0BETAA[Q_,S_]=BESSELJ[0,BETAA[Q,S]];
J1BETAA[Q_,S_]=BESSELJ[1,BETAA[Q,S]];
J0BETAB[Q_,S_]=BESSELJ[0,BETAB[Q,S]];
J1BETAB[Q_,S_]=BESSELJ[1,BETAB[Q,S]];

Y0ALFAA[Q_,S_]=BESSELY[0,ALFAA[Q,S]];
Y1ALFAA[Q_,S_]=BESSELY[1,ALFAA[Q,S]];
Y0ALFAB[Q_,S_]=BESSELY[0,ALFAB[Q,S]];
Y1ALFAB[Q_,S_]=BESSELY[1,ALFAB[Q,S]];
Y0BETAA[Q_,S_]=BESSELY[0,BETAA[Q,S]];
Y1BETAA[Q_,S_]=BESSELY[1,BETAA[Q,S]];
Y0BETAB[Q_,S_]=BESSELY[0,BETAB[Q,S]];
Y1BETAB[Q_,S_]=BESSELY[1,BETAB[Q,S]];

D11[Q_,S_]=(S^2-Q^2/2)*J0ALFAA[Q,S]+ALFAA[Q,S]*J1ALFAA[Q,S];
D12[Q_,S_]=(S^2-Q^2/2)*Y0ALFAA[Q,S]+ALFAA[Q,S]*Y1ALFAA[Q,S];
D13[Q_,S_]=S*(BETAA[Q,S]*J0BETAA[Q,S]-J1BETAA[Q,S]);
D14[Q_,S_]=S*(BETAA[Q,S]*Y0BETAA[Q,S]-Y1BETAA[Q,S]);

D21[Q_,S_]=-2*S*(ALFAA[Q,S]*J1ALFAA[Q,S]);
D22[Q_,S_]=-2*S*(ALFAA[Q,S]*Y1ALFAA[Q,S]);
D23[Q_,S_]=(2*S^2-Q^2)*J1BETAA[Q,S];
D24[Q_,S_]=(2*S^2-Q^2)*Y1BETAA[Q,S];

D31[Q_,S_]=R^2*(S^2-Q^2/2)*J0ALFAB[Q,S]+ALFAB[Q,S]*J1ALFAB[Q,S];
D32[Q_,S_]=R^2*(S^2-Q^2/2)*Y0ALFAB[Q,S]+ALFAB[Q,S]*Y1ALFAB[Q,S];
D33[Q_,S_]=(S*R)*(BETAB[Q,S]*J0BETAB[Q,S]-J1BETAB[Q,S]);
D34[Q_,S_]=(S*R)*(BETAB[Q,S]*Y0BETAB[Q,S]-Y1BETAB[Q,S]);

D41[Q_,S_]=-2*(S*R)*(ALFAB[Q,S]*J1ALFAB[Q,S]);
D42[Q_,S_]=-2*(S*R)*(ALFAB[Q,S]*Y1ALFAB[Q,S]);
D43[Q_,S_]=R^2*(2*S^2-Q^2)*J1BETAB[Q,S];
D44[Q_,S_]=R^2*(2*S^2-Q^2)*Y1BETAB[Q,S];

DN[Q_,S_]=D12[Q,S]*D23[Q,S]*D44[Q,S]-D12[Q,S]*D24[Q,S]*D43[Q,S]-
          D22[Q,S]*D13[Q,S]*D44[Q,S]+D22[Q,S]*D14[Q,S]*D43[Q,S]+
          D42[Q,S]*D13[Q,S]*D24[Q,S]-D42[Q,S]*D14[Q,S]*D23[Q,S];

D1N[Q_,S_]=D11[Q,S]*D23[Q,S]*D44[Q,S]-D11[Q,S]*D24[Q,S]*D43[Q,S]-
           D21[Q,S]*D13[Q,S]*D44[Q,S]+D21[Q,S]*D14[Q,S]*D43[Q,S]+
           D41[Q,S]*D13[Q,S]*D24[Q,S]-D41[Q,S]*D14[Q,S]*D23[Q,S];

D2N[Q_,S_]=D12[Q,S]*D21[Q,S]*D44[Q,S]-D12[Q,S]*D24[Q,S]*D41[Q,S]-
           D22[Q,S]*D11[Q,S]*D44[Q,S]+D22[Q,S]*D14[Q,S]*D41[Q,S]+
           D42[Q,S]*D11[Q,S]*D24[Q,S]-D42[Q,S]*D14[Q,S]*D21[Q,S];

D3N[Q_,S_]=D12[Q,S]*D23[Q,S]*D41[Q,S]-D12[Q,S]*D21[Q,S]*D43[Q,S]-
           D22[Q,S]*D13[Q,S]*D41[Q,S]+D22[Q,S]*D11[Q,S]*D43[Q,S]+
           D42[Q,S]*D13[Q,S]*D21[Q,S]-D42[Q,S]*D11[Q,S]*D23[Q,S];

K1B[Q_,S_,LN_]=COS[S*LN]*(K*ALFAA[Q,S]^2*J0ALFAB[Q,S]+
               K*S^2*J0ALFAB[Q,S]+2*S^2*J0ALFAB[Q,S]);
K2B[Q_,S_,LN_]=COS[S*LN]*(K*ALFAA[Q,S]^2*Y0ALFAB[Q,S]+
               K*S^2*Y0ALFAB[Q,S]+2*S^2*Y0ALFAB[Q,S]);
```

```
K3B[Q_,S_,LN_]=2*COS[S*LN]*S*BETAA[Q,S]*J0BETAB[Q,S];
K4B[Q_,S_,LN_]=2*COS[S*LN]*S*BETAA[Q,S]*Y0BETAB[Q,S];

K1A[Q_,S_,LN_]=COS[S*LN]*(K*ALFAA[Q,S]^2*J0ALFAA[Q,S]+
               K*S^2*J0ALFAA[Q,S]+2*S^2*J0ALFAA[Q,S]);
K2A[Q_,S_,LN_]=COS[S*LN]*(K*ALFAA[Q,S]^2*Y0ALFAA[Q,S]+
               K*S^2*Y0ALFAA[Q,S]+2*S^2*Y0ALFAA[Q,S]);
K3A[Q_,S_,LN_]=2*COS[S*LN]*S*BETAA[Q,S]*J0BETAA[Q,S];
K4A[Q_,S_,LN_]=2*COS[S*LN]*S*BETAA[Q,S]*Y0BETAA[Q,S];

K1AB[Q_,S_,LN_]=COS[S*LN]*(K*ALFAA[Q,S]^2*BESSELJ[0,(ALFAA[Q,S]+3*ALFAB[Q,S])
                /4]+K*S^2*BESSELJ[0,(ALFAA[Q,S]+3*ALFAB[Q,S])/4]+2*S^2*
                BESSELJ[0,(ALFAA[Q,S]+3*ALFAB[Q,S])/4]);
K2AB[Q_,S_,LN_]=COS[S*LN]*(K*ALFAA[Q,S]^2*BESSELY[0,(ALFAA[Q,S]+3*ALFAB[Q,S])
                /4]+K*S^2*BESSELY[0,(ALFAA[Q,S]+3*ALFAB[Q,S])/4]+2*S^2*
                BESSELY[0,(ALFAA[Q,S]+3*ALFAB[Q,S])/4]);
K3AB[Q_,S_,LN_]=2*COS[S*LN]*S*BETAA[Q,S]*BESSELJ[0,(BETAA[Q,S]+3*
                BETAB[Q,S])/4];
K4AB[Q_,S_,LN_]=2*COS[S*LN]*S*BETAA[Q,S]*BESSELY[0,(BETAA[Q,S]+3*
                BETAB[Q,S])/4];

K1ABC[Q_,S_,LN_]=COS[S*LN]*(K*ALFAA[Q,S]^2*BESSELJ[0,(ALFAA[Q,S]+ALFAB[Q,S])/
                 2]+K*S^2*BESSELJ[0,(ALFAA[Q,S]+ALFAB[Q,S])/2]+2*S^2*
                 BESSELJ[0,(ALFAA[Q,S]+ALFAB[Q,S])/2]);
K2ABC[Q_,S_,LN_]=COS[S*LN]*(K*ALFAA[Q,S]^2*BESSELY[0,(ALFAA[Q,S]+ALFAB[Q,S])/
                 2]+K*S^2*BESSELY[0,(ALFAA[Q,S]+ALFAB[Q,S])/2]+2*S^2*
                 BESSELY[0,(ALFAA[Q,S]+ALFAB[Q,S])/2]);
K3ABC[Q_,S_,LN_]=2*COS[S*LN]*S*BETAA[Q,S]*BESSELJ[0,(BETAA[Q,S]+
                 BETAB[Q,S])/2];
K4ABC[Q_,S_,LN_]=2*COS[S*LN]*S*BETAA[Q,S]*BESSELY[0,(BETAA[Q,S]+
                 BETAB[Q,S])/2];

K1ABCD[Q_,S_,LN_]=COS[S*LN]*(K*ALFAA[Q,S]^2*BESSELJ[0,(3*ALFAA[Q,S]+
                  ALFAB[Q,S])/4]+K*S^2*BESSELJ[0,(3*ALFAA[Q,S]+ALFAB[Q,S])/4]
                  +2*S^2*BESSELJ[0,(3*ALFAA[Q,S]+ALFAB[Q,S])/4]);
K2ABCD[Q_,S_,LN_]=COS[S*LN]*(K*ALFAA[Q,S]^2*BESSELY[0,(3*ALFAA[Q,S]+
                  ALFAB[Q,S])/4]+K*S^2*BESSELY[0,(3*ALFAA[Q,S]+ALFAB[Q,S])/4]
                  +2*S^2*BESSELY[0,(3*ALFAA[Q,S]+ALFAB[Q,S])/4]);
K3ABCD[Q_,S_,LN_]=2*COS[S*LN]*S*BETAA[Q,S]*BESSELJ[0,(3*BETAA[Q,S]+
                  BETAB[Q,S])/4];
K4ABCD[Q_,S_,LN_]=2*COS[S*LN]*S*BETAA[Q,S]*BESSELY[0,(3*BETAA[Q,S]+
                  BETAB[Q,S])/4];

P1A[Q_,S_,LN_]=-2*SIN[S*LN]*S*BESSELJ[1,(ALFAA[Q,S]+4*ALFAB[Q,S])/5]*
               ALFAA[Q,S];
P2A[Q_,S_,LN_]=-2*SIN[S*LN]*S*BESSELY[1,(ALFAA[Q,S]+4*ALFAB[Q,S])/5]*
               ALFAA[Q,S];
P3A[Q_,S_,LN_]=-SIN[S*LN]*BESSELJ[1,(BETAA[Q,S]+4*BETAB[Q,S])/5]*
               (-S^2+BETAA[Q,S]^2);
P4A[Q_,S_,LN_]=-SIN[S*LN]*BESSELY[1,(BETAA[Q,S]+4*BETAB[Q,S])/5]*
               (-S^2+BETAA[Q,S]^2);

P1B[Q_,S_,LN_]=-2*SIN[S*LN]*S*BESSELJ[1,(2*ALFAA[Q,S]+3*ALFAB[Q,S])/5]*
               ALFAA[Q,S];
P2B[Q_,S_,LN_]=-2*SIN[S*LN]*S*BESSELY[1,(2*ALFAA[Q,S]+3*ALFAB[Q,S])/5]*
               ALFAA[Q,S];
P3B[Q_,S_,LN_]=-SIN[S*LN]*BESSELJ[1,(2*BETAA[Q,S]+3*BETAB[Q,S])/5]*
               (-S^2+BETAA[Q,S]^2);
P4B[Q_,S_,LN_]=-SIN[S*LN]*BESSELY[1,(2*BETAA[Q,S]+3*BETAB[Q,S])/5]*
               (-S^2+BETAA[Q,S]^2);

P1C[Q_,S_,LN_]=-2*SIN[S*LN]*S*BESSELJ[1,(3*ALFAA[Q,S]+2*ALFAB[Q,S])/5]*
               ALFAA[Q,S];
P2C[Q_,S_,LN_]=-2*SIN[S*LN]*S*BESSELY[1,(3*ALFAA[Q,S]+2*ALFAB[Q,S])/5]*
```

```
                ALFAA[Q,S];
P3C[Q_,S_,LN_]=-SIN[S*LN]*BESSELJ[1,(3*BETAA[Q,S]+2*BETAB[Q,S])/5]*
                (-S^2+BETAA[Q,S]^2);
P4C[Q_,S_,LN_]=-SIN[S*LN]*BESSELY[1,(3*BETAA[Q,S]+2*BETAB[Q,S])/5]*
                (-S^2+BETAA[Q,S]^2);

P1D[Q_,S_,LN_]=-2*SIN[S*LN]*S*BESSELJ[1,(4*ALFAA[Q,S]+ALFAB[Q,S])/5]*
                ALFAA[Q,S];
P2D[Q_,S_,LN_]=-2*SIN[S*LN]*S*BESSELY[1,(4*ALFAA[Q,S]+ALFAB[Q,S])/5]*
                ALFAA[Q,S];
P3D[Q_,S_,LN_]=-SIN[S*LN]*BESSELJ[1,(4*BETAA[Q,S]+BETAB[Q,S])/5]*
                (-S^2+BETAA[Q,S]^2);
P4D[Q_,S_,LN_]=-SIN[S*LN]*BESSELY[1,(4*BETAA[Q,S]+BETAB[Q,S])/5]*
                (-S^2+BETAA[Q,S]^2);

SIGMAZ1[Q_,S_,LN_]=K1B[Q,S,LN]-K2B[Q,S,LN]*(D1N[Q,S]/DN[Q,S])-K3B[Q,S,LN]*
                   (D2N[Q,S]/DN[Q,S])-K4B[Q,S,LN]*(D3N[Q,S]/DN[Q,S]);

SIGMAZ2[Q_,S_,LN_]=K1A[Q,S,LN]-K2A[Q,S,LN]*(D1N[Q,S]/DN[Q,S])-K3A[Q,S,LN]*
                   (D2N[Q,S]/DN[Q,S])-K4A[Q,S,LN]*(D3N[Q,S]/DN[Q,S]);

SIGMAZ3[Q_,S_,LN_]=K1AB[Q,S,LN]-K2AB[Q,S,LN]*(D1N[Q,S]/DN[Q,S])-K3AB[Q,S,LN]*
                   (D2N[Q,S]/DN[Q,S])-K4AB[Q,S,LN]*(D3N[Q,S]/DN[Q,S]);

SIGMAZ4[Q_,S_,LN_]=K1ABC[Q,S,LN]-K2ABC[Q,S,LN]*(D1N[Q,S]/DN[Q,S])-
           K3ABC[Q,S,LN]*(D2N[Q,S]/DN[Q,S])-K4ABC[Q,S,LN]*(D3N[Q,S]/DN[Q,S]);

SIGMAZ5[Q_,S_,LN_]=K1ABCD[Q,S,LN]-K2ABCD[Q,S,LN]*(D1N[Q,S]/DN[Q,S])-
         K3ABCD[Q,S,LN]*(D2N[Q,S]/DN[Q,S])-K4ABCD[Q,S,LN]*(D3N[Q,S]/DN[Q,S]);

TAURZ1[Q_,S_,LN_]=P1A[Q,S,LN]-P2A[Q,S,LN]*(D1N[Q,S]/DN[Q,S])-P3A[Q,S,LN]*
                  (D2N[Q,S]/DN[Q,S])-P4A[Q,S,LN]*(D3N[Q,S]/DN[Q,S]);

TAURZ2[Q_,S_,LN_]=P1B[Q,S,LN]-P2B[Q,S,LN]*(D1N[Q,S]/DN[Q,S])-P3B[Q,S,LN]*
                  (D2N[Q,S]/DN[Q,S])-P4B[Q,S,LN]*(D3N[Q,S]/DN[Q,S]);

TAURZ3[Q_,S_,LN_]=P1C[Q,S,LN]-P2C[Q,S,LN]*(D1N[Q,S]/DN[Q,S])-P3C[Q,S,LN]*
                  (D2N[Q,S]/DN[Q,S])-P4C[Q,S,LN]*(D3N[Q,S]/DN[Q,S]);

TAURZ4[Q_,S_,LN_]=P1D[Q,S,LN]-P2D[Q,S,LN]*(D1N[Q,S]/DN[Q,S])-P3D[Q,S,LN]*
                  (D2N[Q,S]/DN[Q,S])-P4D[Q,S,LN]*(D3N[Q,S]/DN[Q,S]);

Q1=TABLE[M,{M,0.81,10.02,0.03}];

(* REAL, IMAGINARY AND COMPLEX ZEROS OBTAINED IN APPENDIX I *)
PART1={0.49868117163553, ... 10.77636905728296};
PART2={1.513432173414966 + 2.405820364411799*I, ... 9.39797659996387};
PART3={1.513432173414966 - 2.405820364411799*I, ... 5.82159149336508};
PART4={2.735801199888889 + 5.871945862922929*I, ... 4.92102464118514};
PART5={2.735801199888889 - 5.871945862922929*I, ... 1.65881166523624};
PART6={3.445062420004788 + 9.71044173350448*I, ...
       3.198850344825034 + 5.523581062986799*I};
PART7={3.445062420004788 - 9.71044173350448*I, ...
       3.198850344825034 - 5.523581062986799*I};
PART8={3.879941470077832 + 13.61547250712715*I, ...
       3.87877673266707 + 11.02895351069916*I};
PART9={3.879941470077832 - 13.61547250712715*I, ...
       3.87877673266707 - 11.02895351069916*I};

S1={ PART1,PART2,PART3,PART4,PART5,PART6,PART7,PART8,PART9};
S2=TABLE[TRANSPOSE[S1]];

N=LENGTH[Q1];
DIMENSIONS[S1];
```

```
DIMENSIONS[S2];

DELTA=0;

(*INITIAL VALUE*)
P=3.6;

T=TABLE[0,{N}];
FOR[I=1, I<=N, I++,
Q=Q1[[I]];
S=S2[[I]];
A1[LN_]=SIGMAZ1[Q,S,LN];
A2[LN_]=SIGMAZ2[Q,S,LN];
A3[LN_]=SIGMAZ3[Q,S,LN];
A4[LN_]=SIGMAZ4[Q,S,LN];
A5[LN_]=SIGMAZ5[Q,S,LN];
A6[LN_]=TAURZ1[Q,S,LN];
A7[LN_]=TAURZ2[Q,S,LN];
A8[LN_]=TAURZ3[Q,S,LN];
A9[LN_]=TAURZ4[Q,S,LN];
YY[LN_]=TABLE[{A1[LN],A2[LN],A3[LN],A4[LN],A5[LN],A6[LN],
A7[LN],A8[LN],A9[LN]}];
Y[LN_]=DET[YY[LN]];
R=FINDROOT[Y[LN]==0,{LN,P}];
P1=LN/.R;
P=RE[P1];
P>>>D:\RESULTS;
PRINT[P1];
T[[I]]=P1;
];
```

REFERENCES

1. A.Iula, N.Lamberti, R.Carotenuto, M.Pappalardo, *A 3-D model of the classical Langevin transducer*, IEEE 1997 Ultrasonics Symposium Proceedings, pp. 987÷990, Oct. 1997.
2. R.Kumar, *Dispersion of Axially Symmetric Waves in Empty and Fluid-Filled Cylindrical Shells*, Acustica, vol. 27, pp. 317÷329, 1972.
3. I.Malecki, *Physical foundations of technical acoustics,* Pergamon Press, Oxford, 1969.
4. R.Kumar, *Axially Symmetric Vibrations of Finite Cylindrical Shells of Various Wall Thicknesses*, Acustica, vol. 34, pp. 281÷288, 1976.
5. J.Van Randeraat, R.E.Setterington, *Piezoelectric ceramics*, Elcoma Technical Publications Department, Philips, Eindhoven, 1974.
6. *Five piezoelectric ceramics*, Bulletin 66011/F, Vernitron Ltd., 1976.
7. D.Mančić, V.Dimić, M.Radmanović, *Resonance frequencies of PZT piezoceramic disks: a numerical approach*, Facta Universitatis, Series Mechanics, Automatic Control and Robotics, vol. 3, no. 12, pp. 431÷442, 2002.

NUMERIČKI PRISTUP U ANALIZI OSNOSIMETRIČNIH PRSTENOVA

Dragan Mančić, Milan Radmanović

U ovom radu primenom tačnih trodimenzionalnih jednačina linearne elastičnosti analizirane su osnosimetrične oscilacije konačnih čvrstih kružnih prstenova sa različitim otvorom i dužinom. Realne, imaginarne i kompleksne grane odgovarajućeg disperzionog spektra, dobijene tačnim zadovoljavanjem graničnih uslova sa nultim naponima na kružnim površinama prstena, superponirane su da aproksimativno zadovolje granične uslove sa nultim naponima na ravnim površinama prstena. Postupak superpozicije dovodi do transcedentne jednačine, koja daje zavisnosti između frekvencije i dužine prstena. Ove zavisnosti su prikazane za prstenove od različitih materijala i za različito odabrane dimenzije.